Available online at www.sciencedirect.com

jmr&t Journal of Materials Research and Technology

https://www.journals.elsevier.com/journal-of-materials-research-and-technology

Original Article

Studying and spectral characterization for the separation of lanthanides from phosphate ore by organic and inorganic acids

A.A. Nayl[a,b,*], W.A.A. Arafa[a,c], A.I. Abd-Elhamid[d], R.A. Elkhashab[a,e]

[a] Chemistry Department, College of Science, Jouf University, P.O. Box 2014, Sakaka, Aljouf, Kingdom of Saudi Arabia
[b] Hot Laboratories Center, Atomic Energy Authority of Egypt, P.O. Box 13759, Cairo, Egypt
[c] Chemistry Department, Faculty of Science, Fayoum University, P.O. 63514, Fayoum City, Egypt
[d] Advanced Technology and New Materials Research Institute, City of Scientific Research and Technological Applications (SRTA-City), New Borg Al-Arab, Alexandria 21934, Egypt
[e] National Center for Clinical and Environmental Toxicology, Faculty of Medicine, Cairo University, Cairo, Egypt

ARTICLE INFO

Article history:
Received 2 March 2020
Accepted 5 July 2020
Available online 29 July 2020

Keywords:
Phosphate ore
Acid leaching
Lanthanides
Kinetic model

ABSTRACT

In this study, the separation of lanthanides from phosphate ore using oxalic acid ($C_2H_2O_4$), tartaric acid ($C_4H_6O_6$), lactic acid ($C_3H_6O_3$), sulfuric acid (H_2SO_4) and hydrochloric acid (HCl) was investigated. The ore was characterized before and after leaching processes by X-ray fluorescence (XRF), Scanning electron microscope (SEM), X-ray powder diffraction (XRD), and Fourier transform infrared (FTIR). The different parameters affect the leaching rate such as leaching time, acid concentration, liquid/solid ratios, temperature, and leaching kinetics were studied. The optimal leaching conditions were determined as 0.4 M $C_2H_2O_4$, 2.5 M $C_4H_6O_6$, 1.8 M $C_3H_6O_3$, 2.0 M H_2SO_4, and 3.0 M HCl, with a liquid/solid (L/S) mass ratio of 6/1 $C_2H_2O_4$, 8/1 for both $C_4H_6O_6$ and $C_3H_6O_3$, 5/1 for both H_2SO_4 and HCl at 30 °C, agitation rate ≈ 350 rpm and particle size ≈ 144.8 μm. Under these optimum conditions, the recovery percentage (%R) was 42.8% (for $C_2H_2O_4$), 93.2% (for $C_4H_6O_6$), 89.1% (for $C_3H_6O_3$), 89.3% (for H_2SO_4), and 74.6% (for HCl). SEM and FTIR characterizations for the residue were investigated. Experimental data reveal that the leaching processes are fitted by chemical reaction models for $C_2H_2O_4$ and $C_3H_6O_3$, and by diffusion-reaction model for $C_4H_6O_6$, H_2SO_4, and HCl. The activation energies for these models were estimated to be 43.3, 30.33, 45.8, 31.3, and 38.6 kJ/mol for $C_2H_2O_4$, $C_4H_6O_6$, $C_3H_6O_3$, H_2SO_4, and HCl, respectively. All data were confirmed and explained by XRD, FTIR, and SEM studies.

1. Introduction

In recent decades, the demand for lanthanide elements has been increasing as they have unique chemical and physi-

* Corresponding author.
E-mails: aanayl@yahoo.com, aanayel@ju.edu.sa (A. Nayl).
https://doi.org/10.1016/j.jmrt.2020.07.007

cal properties suitable for applications in advanced materials. Indeed, they have a high techno-economic interest and a large variety of modern technological applications such as optics, catalysis, alloys, electronics tools, superconductor technologies, advanced weapons systems, and nuclear technologies [1–4]. Due to the unique properties of these elements, a great attention is directed to develop their effectiveness and environmentally separation techniques from their sources. There is a wide variety of ores, minerals, and low-grade ores known as sources for lanthanide elements [5]. Lanthanides occur in more than 160 discrete ores. Most of these ores are considered as sources hosting lanthanides, such as bastnesite (La, Ce)FCO_3, monazite, (Ce, La, Y, Th)PO_4, and apatite, where the lanthanides that are associated with other elements and their contents are expressed as oxide [6]. The general chemical formula of apatite is $Ca_5(PO_4)_3X$, where X is Cl^- or F^- or OH^-. Phosphate ores are regarded as fluorapatite ore [$Ca_5(PO_4)_3F$] and contain an average of 0.1–0.8% lanthanide oxides [7].

Ores containing lanthanides are usually processed by either physical concentration or leaching processes [8]. Physical concentration processes include ore crushing and then separating the lanthanides as oxides by physical methods. This process is successful only if the amount of lanthanides in the ore is considerable, such as monazite and bastnäsite [9]. For low-grade phosphate ores, acidic or alkaline leaching processes are more suitable methods to recover the lanthanides. Recently, different approaches for leaching of lanthanides from its ores by different mineral acids have been published where some of these sources are usually concentrated and leached in HCl, H_2SO_4, $HClO_4$, HCl, HNO_3 and H_3PO_4 solutions [10–14]. When H_2SO_4 is used as a leachant, large amounts of lanthanides are recovered and precipitated with phosphorgypsum. Also, the recovery of lanthanides using HNO_3 and HCl leaching systems was more than that reported using H_3PO_4 solution [10–14]. As reported in the literature, the ores were dissolved well in HCl or HNO_3, but it was only attacked with concentrated H_2SO_4 at high temperatures [10,12,13]. However, due to the complex metallurgy of lanthanides, there is no standard method for dissolution lanthanides-bearing ores [7,15–17]. Leaching processes by such mineral acid lead to erosion of the processing facilities, co-separation of considerable proportions of other undesirable impurities and toxic waste streams. Therefore the extraction of lanthanides from such leachant is complicated and costly. So, organic acid leaching of phosphate ores has been investigated and studied to leach the low-grade ores [17–22].

Generally, lanthanides are present in phosphate ores as ionic substitutions in the crystal lattice with Ca [23]. However, there is no standard technique known for the recovery of lanthanides-containing ores due to the nature of the complex metallurgy of lanthanides and their chemical similarity [8]. Although using organic acids to leach the calcareous phosphate ores can be considered as promising leaching reagents, there are some advantages and disadvantages that should be taken into consideration in these leaching processes [19,20]. The advantages of these leaching reagents are then few environmental hazards, very selective, low cost, recyclability, and reprocessing of the leachant, and the disadvantage is that the economic aspects are not well-established [19].

In Saudi Arabia, the total resources of the phosphate ore at the AI-Jalamid Mine and at the Sirhan-Turayf, located in Northern Saudi Arabia, are about 500 and 7800 mmt, respectively, with about 19.5% P_2O_5. Therefore, the phosphate ores in these areas are considered as one of the most promising phosphate ore in the kingdom [24,25]. The main disadvantage of such a carbonaceous sedimentary type of phosphate ore all over the world is its high carbonate content [26]. So, calcination processes are used in such areas that have a shortage of water resources and low-cost energy. On the other hand, Al-Jalamid phosphate deposits contain about 16–25% P_2O_5, 40–50% carbonate, and 8–10% organic substances. To remove lime, the ore is calcinated to 850 °C for 1 h, followed by washing with water, then quenching to remove magnesium using 5% NH_4NO_3 [27,28]. In phosphate ore, lanthanides are present in isomorphous substitution form with calcium and deposit as the lanthanides-francolite that can be leached with acids into the aqueous phase [29].

Although the history of leaching and separation of lanthanides from such ores dates back to the 1930s [29]. The investigations regarding the spectral characterization of the leaching of lanthanide elements from phosphate ore by organic acids are limited in the literature. Thus, this work is aimed to study and characterize the leaching processes of lanthanides from phosphate ore by some organic and inorganic acids. Due to the harmful effects of using mineral acids in these leaching processes, our work is directed to develop the leaching of lanthanides from phosphate ore by some organic acids to overcome the economic and environmental drawbacks of using mineral acids, and compare the results with other investigated inorganic acids. All results obtained for both investigated organic and inorganic acids have been characterized and compared.

In the light of the above-mentioned considerations, the main objective of our work has been oriented to characterize and study the leaching of lanthanides from Al-Jalamid phosphate ore, using organic and inorganic acids such as; $C_2H_2O_4$, $C_4H_6O_6$, $C_3H_6O_3$, H_2SO_4, and HCl. The factors that affect the investigated leaching processes as, leaching time, acid concentration, liquid/solid mass ratios, and leaching temperature were studied. The kinetic studies for the leaching processes were optimized.

2. Experimental

2.1. Materials

The samples of phosphate ores used in this work were obtained from phosphate deposits in Al-Jalamid region, Saudi Arabia. The chemical compositions of the phosphate ore before and after leaching were determined by energy dispersive X-ray fluorescence (EDS) spectrometer Model; OXFORD attached with SEM Model JSM-6510 series. Table 1 shows the bulk chemical composition of the phosphate ore. All the chemicals used in the leaching processes and determinations were of analytical grade and used without any further purifications. The chemical structures of the investigated organic acids (oxalic, tartaric, and lactic acid) are represented in Fig. 1.

Table 1 – Bulk chemical composition of (Al-Jalamid) phosphate ore.

Element	SiO_2	Al_2O_3	$Fe_2O_3{}^{Tot}$	MgO	CaO	Na_2O	K_2O	P_2O_5	SO_3	F	LOI[a]	SrO	ZrO_2	Y_2O_3
wt.%	2.26	0.10	0.12	0.63	58.29	0.18	0.02	27.30	1.10	0.74	9.21	0.05	0.01	0.01

[a] LOI = Loss of ignition.

Table 2 – Chemical analysis of lanthanides in phosphate ore.

Element	Ce	La	Pr	Nd	Sm	Eu	Y	Gd	Tb	Dy	Er	Ho	Yb	Lu	Tm	Sc
Conc. (ppm)	73.5	59.0	10.0	54.9	3.8	2.5	74.3	11.2	8.8	11.6	16.6	4.7	13.7	1.2	2.0	5.5

2.2. *Chemical analysis*

X-ray fluorescence (XRF, Philips PW 2404) was used to determine the overall chemical compositions of the phosphate samples and its residues; the samples were analyzed by pressed powder pellets.

The mineralogical analysis of the phosphate samples and its residues was carried out by XRD-7000S high-resolution X-ray diffractometer instrument.

Fourier transform infrared (FTIR) spectroscopy was performed Shimadzu IR Tracer and the scan was performed from 400 to 4000 cm^{-1}.

The analysis of the lanthanide elements concentrations in the phosphate ore and residues were measured by an atomic absorption spectrophotometer, Model S Series, Thermo-electron Corporation (Table 2), and the total lanthanide elements concentrations were measured spectrophotometrically in the leaching solutions by using Arsenazo (III) method [30].

2.3. *Particle-size analysis*

The phosphate sample was mechanically crushed till reached a given particle size. Particle-size distributions were determined using the wet-sieve (AFNOR) method (0.01–2800 Microns size ranges) using Blue Laser Diffraction Particle Size Analyzer, BLUEWAVE. Binocular observation of the different size fractions of the sample was used to identify and quantify, by visual inspection and grain counting, the relative percentages of the major minerals, and to evaluate the release mesh of phosphate minerals.

2.4. *Leaching procedures*

The used phosphate ore sample was collected from Al-Jalamid site, KSA. Particle size fraction less than 144.8 μm was used in all studies. Firstly, the sample was washed by double distilled water to remove the soluble materials and dried in an electric oven at about 105 °C. Then, the dry sample was cooled at room temperature and stored in closed desiccators. Al-Jalamid phosphate ore used in this study contains about 285 ppm of lanthanides.

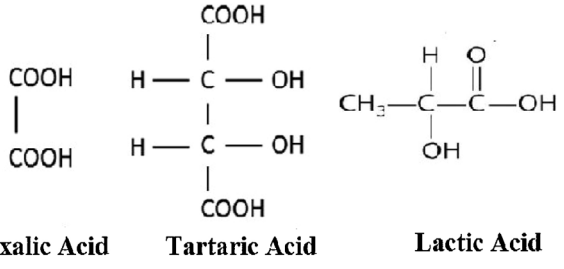

Fig. 1 – Chemical structure of investigated organic acids used in this work.

The leaching experiments were carried out in closed glass flasks by mechanically mixing of 350 rpm with different liquid/solid mass ratios in a thermostatic vessel at different time periods and at 25 °C, unless otherwise cited. At the end of each leaching experiment, the mixture was filtered and the leach liquor was analyzed to calculate the lanthanides recovery percentage (%R).

Based on the data obtained, the leaching conditions were optimized to maximize lanthanides recovery and minimize other contaminants dissolved using the investigated acids.

Also, after each leaching process, the residue remained after filtration was analyzed by, IR, XRD, XRF, and SEM.

All the figures in this work represent the experimental results obtained for lanthanides elements only, unless otherwise stated.

The Arsenazo (III) method is used to determine the total lanthanides in the leaching solution. The method has the advantage that the reagent is not absorbed at the wavelength of the absorption maximum of the complex (λ_{max}=650 nm.).

The procedure used for the determination was as follows;

To the lanthanides solution (pH = 1), add 0.4 cm^3 of 1% ascorbic acid solution. After a few minutes, add 0.2 cm^3 of the formate buffer and 0.8 cm^3 of Arsenazo (III) solutions, and dilute with water to 8 cm^3.

3. Results and discussion

3.1. *Phosphate ore characterization*

3.1.1. *Particle size analyze*

The particle size distribution curve of the phosphate ore sample is illustrated in Fig. 2, and showed a unimodal pattern with an approximately normal distribution. The data obtained shows that the sample is composed of small particle size and this leads to an increase in the interfacial area of phosphate-acid that can occur either by decreasing the particle size or increasing the porosity of ore sample. The increase in the phosphate- acid interfacial area would contribute to the improved lanthanides' dissolution processes [31]. Therefore, the average particle size fraction of the phosphate particles under 144.8 μm was used in this study.

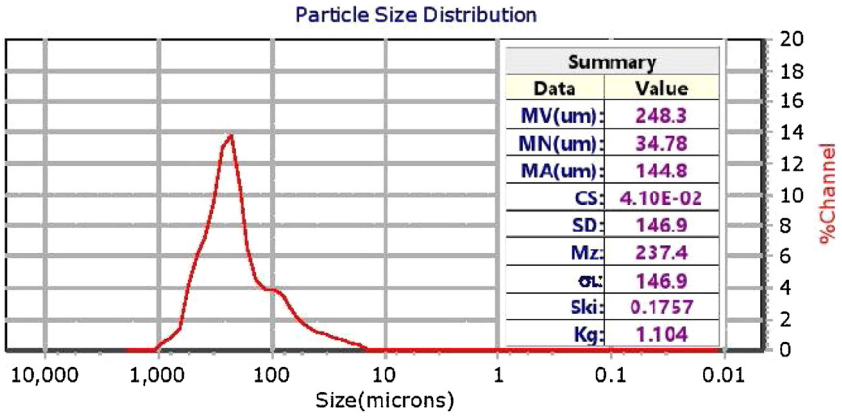

Fig. 2 – The particle size distribution of the phosphate ore. Where, MV is the Mean diameter in microns of the "volume distribution", MN is the Mean diameter, in microns, of the "number distribution", MA is the Mean diameter, in microns, of the "area distribution", CS is the Calculated surface – Provided in units of M^2/cc, SD is the Standard Deviation in microns, Mz is the Graphic Mean provides a less coarse-particle weighted mean particle size than MV, σi is the Inclusive Graphic Standard Deviation, Ski is the Inclusive Graphic Skewness, KG - Often known as SKg- Kurtosis (peakedness) of a distribution.

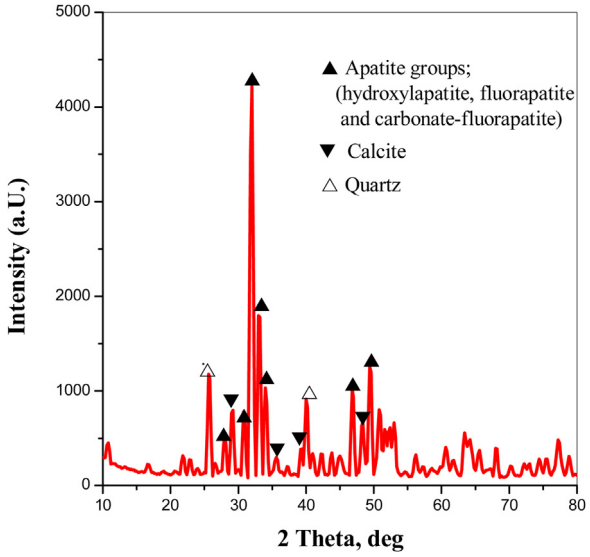

Fig. 3 – X-Ray Diffraction Analysis for Al Jalamid phosphate ore.

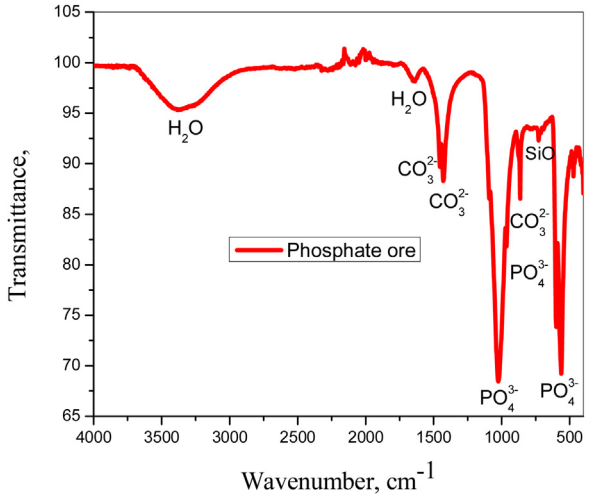

Fig. 4 – FTIR spectra of the Al-Jalamide phosphate ore.

3.1.2. *X-ray diffraction*

The structure of the phosphate ore sample was characterized using the X-ray diffraction, as presented in Fig. 3. The obtained XRD diffraction patterns showed that the phosphate sample includes calcite, quartz, and the carbonate fluorapatite (CFA) that is the main constituent of Al-Jalamide phosphate ore. Where, the observed main bands at (2θ) 28.01 ° and 31.94° that followed by two high-intensity bands between 33.1°-34.2° may be due to apatite groups (hydroxylapatite, fluorapatite and carbonate-fluorapatite) [32,33]. Other distinct main bands at (2θ) 29.1°, 39.3°, 40°, 49.4° belong to calcite which is the main constituent in the phosphate ore [32]. Quartz SiO_2 bands at (2θ) 25.73°, 40.1°. These results agreed and confirming the results obtained by XRF analysis (as in Table 1).

3.1.3. *FTIR analysis*

The obtained infrared spectra of the phosphate ore are illustrated in Fig. 4. The bands observed at about 474.5, 576.7, 964.4, 1045.4 and 1097.5 cm^{-1} are ascribable to PO_4^{3-} groups [33]. The bands appearing at about 868, 1431.2, and 1458.2 cm^{-1} are characterized bands for carbonate CO_3^{2-} groups [34]. The peak observed at 1458.2 cm^{-1} is typical of carbonated fluoroapatite and due to the presence of carbonate [35]. The bands observed at 750.3 and 815.9 cm^{-1} can be attributed to silicates groups' vibration [33]. Bands observed at about 1024, 600, and 563 cm^{-1} may be attributed to the existence of lanthanides in the lattice of the phosphate ore [36]. In addition, the bands appear at 563 and 600 cm^{-1} are due to P—O mode [37]. The bands located at 864, 1429.25 cm^{-1} are characterized bands assigned to the presence of C=O in the calcite [10,35,38]. These bands are strong and proving the presence of significant amounts of calcite in the used phosphate ore. Also, the band appear-

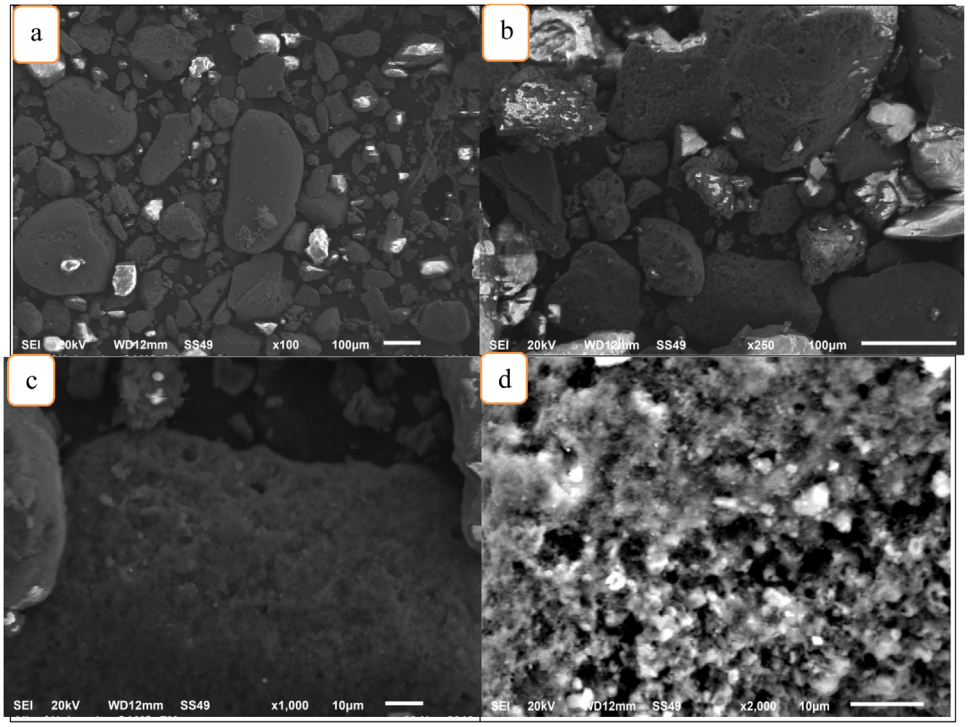

Fig. 5 – Images of SEM of the phosphate ore magnifications of (a)100x, (b)250x, (c)1000x and (d)2000×.

ing at 3373.5 cm^{-1} is assigned to adsorbed H_2O molecules [39]. The results obtained by IR spectra are revealed and agree with that obtained by XRD, and prove the presence of such phases in the used phosphate ore. Therefore, XRD and IR spectra show that the obtained crystal structure of Al-Jalamid phosphate ore consists mainly of fluorapatite mineral and calcite with other minor quartz.

3.1.4. *SEM and EDX of the phosphate ore sample*

SEM micrographs of the powder phosphate ore with different magnifications are investigated, Fig. 5a-d. The data obtained illustrated that the morphology of the phosphate ore is formed mainly by irregular particle forms and a heterogeneous microstructure. The images presented in Fig. 5a revealed that the ore particles are strongly agglomerated and approximately 90% were smaller than 100 μm. Fig. 5a–d shows that, with the magnifications of 100 and 250x, the nearly oval form with a smooth surface is the characterized form the nodules of phosphate [40], Fig. 5a and b. With the magnifications of 1000 and 2000x, Fig. 5c and d, the porosity of the phosphate particle surface becomes clearer, where the pores appeared to cover the entire particle surface.

The EDX spectrum of phosphate ore sample investigated. The data obtained illustrated the mineralogical compositions of the phosphate ore is mainly content fluorapatite and calcite with small quartz [41] with other traces of some elements. From the data reported in Table 1, we can observe that the atomic ratio of $CaO/P_2O_5 = 2.135$ indicates the high content of carbonate in the phosphate ore sample and is agree with that reported in the literature [41]. These results confirmed the results obtained with XRD and IR analysis.

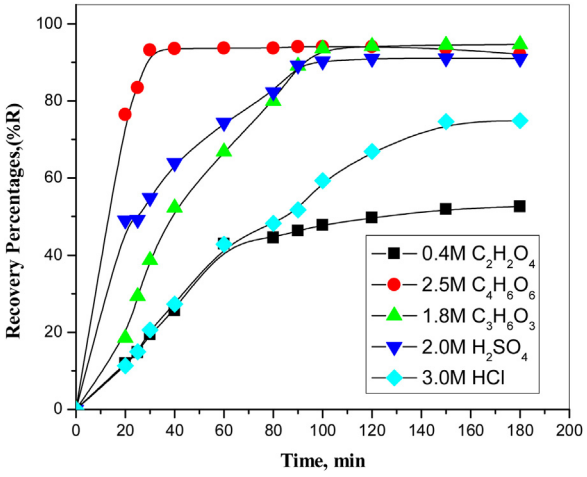

Fig. 6 – Effect of contact time on the leaching of lanthanides from Phosphate ore with some organic and inorganic acids.

3.2. *Leaching process*

3.2.1. *Effect of leaching time*

The effect of time on the dissolution of lanthanides from Al-Jalamid phosphate ore was tested with a period range of 20–180 min. These experiments were carried out by 0.4 M $C_2H_2O_4$, 2.5 M $C_4H_6O_6$, 1.8 M $C_3H_6O_3$, 2.0 M H_2SO_4, and 3.0 M HCl, with L/S mass ratio of 6/1 for $C_2H_2O_4$, 8/1 (for both $C_4H_6O_6$ and $C_3H_6O_3$), and 5/1)for both H_2SO_4 and HCl), at 25 °C (for both $C_2H_2O_4$ and H_2SO_4), and at 35 °C (for $C_4H_6O_6$, $C_3H_6O_3$, and HCl). Fig. 6 shows that the recovery percentage (%R) of lanthanides was increased at the first 30 min to reach 19.4% (for $C_2H_2O_4$),

93.2% (for $C_4H_6O_6$), 38.7 % (for $C_3H_6O_3$), 54.9% (for H_2SO_4), and 20.6 % (HCl), respectively. As the time increase, the (%R) of lanthanides increases to reach 42.9% (at 60 min for $C_2H_2O_4$), 89.1% and 89.3% (at 90 min for both $C_3H_6O_3$ and H_2SO_4, respectively), and 74.6% (at 150 min for HCl), respectively, while the recovery by $C_4H_6O_6$ was remained constant at 93.2%. These results may be attributed to the fact that the leaching of lanthanides from phosphate ore may consist of at least four important steps, (i) hydrolysis of lanthanides, (ii) diffusion of the leaching agent from the main bulk of the solution through the boundary layer to active sites of the phosphate ore, (iii) the nucleation of products at the active sites, and (iv) the hydration of the products and diffusion to the aqueous media. So, these investigated leaching processes are time-dependent processes [42].

Therefore 30 min. (for $C_4H_6O_6$), 60 min. (for $C_2H_2O_4$), 90 min. (for both $C_3H_6O_3$ and H_2SO_4), and 150 min (for HCl) represents the optimum leaching time for maximizing the recovery of lanthanides by the investigated acids and was used in further studies.

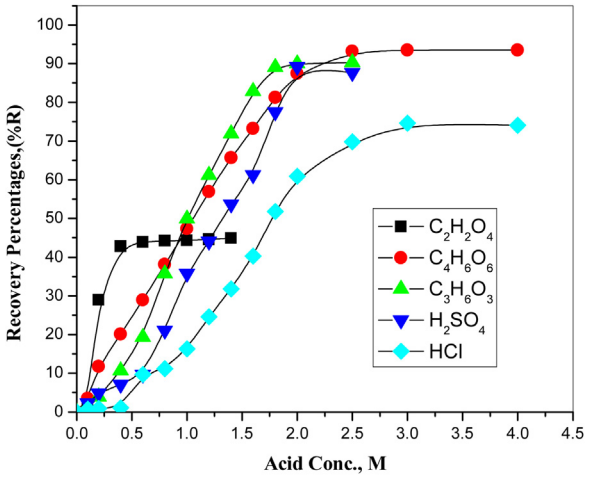

Fig. 7 – Effect of acid concentration on the leaching of lanthanides from phosphate ore.

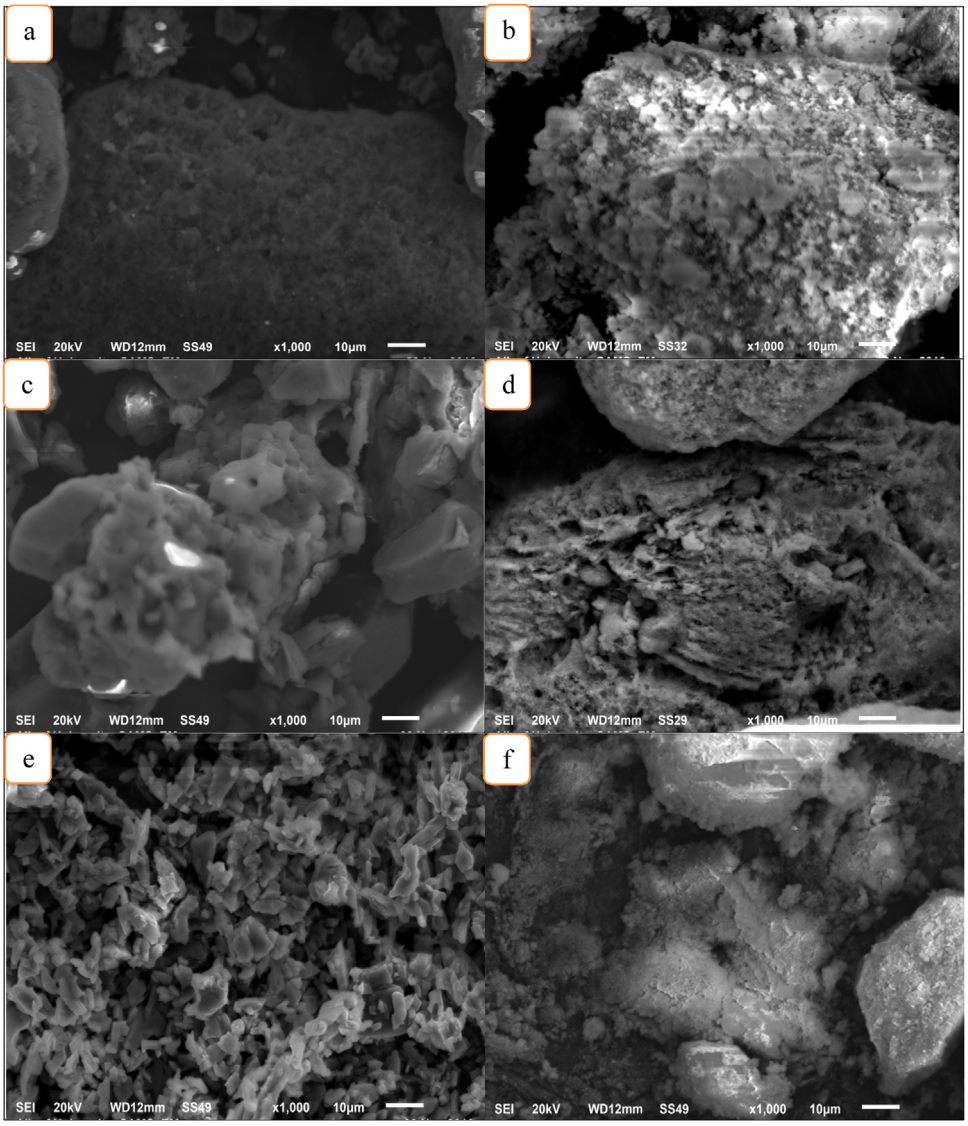

Fig. 8 – Images of SEM of the phosphate ore before and after leaching (residue) (a) phosphate ore before leaching, (b) phosphate ore leached by $C_2H_2O_4$, (c) phosphate ore leached by $C_4H_6O_6$, (d) phosphate ore leached by $C_3H_6O_3$, (e) phosphate ore leached by H_2SO_4, (f) phosphate ore leached by HCl ; magnifications of 1000x.

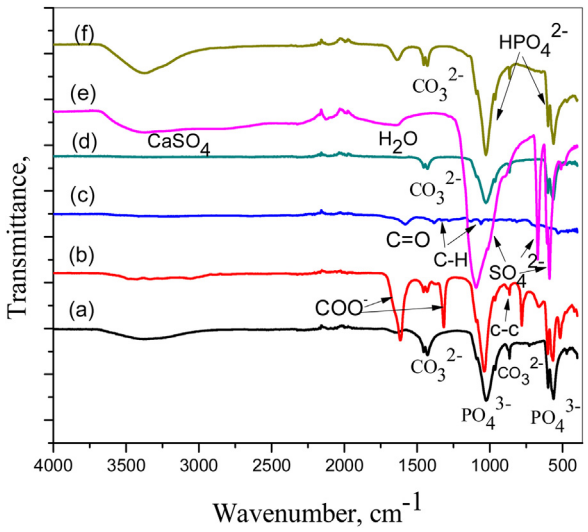

Fig. 9 – FTIR spectra of the Al-Jalamide phosphate ore before and after leaching (residue), (a) phosphate ore before leaching, (b) residue after leaching by $C_2H_2O_4$, (c) residue after leaching by $C_4H_6O_6$, (d) residue after leaching by $C_3H_6O_3$, (e) residue after leaching by H_2SO_4, (f) residue after leaching by HCl.

3.2.2. *Effect of acid concentration*

The influence of acid concentration of $C_2H_2O_4$, $C_4H_6O_6$, $C_3H_6O_3$, H_2SO_4, and HCl, on the leaching of lanthanides was investigated, as in Figs. 7–9.

For $C_2H_2O_4$, different acid concentrations were used (0.1–1.4 M) with L/S mass ratio of 6/1 at 25 °C for 60 min. The data obtained, Fig. 7, shows that the recovery percentage of lanthanides was increased from 2.7% to 42.6% as the acid concentration increases from 0.1–0.4 M. The leaching percentage of lanthanides was increased slowly with further increase in acid concentration to reach 44.9% with 1.4 M $C_2H_2O_4$. While the rate of recovery of other metals, such as Ca under investigated conditions remained constant at about 12.8%. These results may be attributed to the formation of Ca-oxalate and Lanthanide –oxalate precipitates during the leaching processes [42,43]. The mechanism of nonstoichiometric recovery may be attributed to precipitation of metals-containing solids or re-adsorption of these metals to the apatite surface [43]. In this work, as in Fig. 8, the results obtained revealed that the most likely mechanism is re-adsorption of metals to the apatite surface, as shown in the SEM micrograph of the leaching residue, Fig. 8b. Also, the data obtained in FTIR spectra, Fig. 9b, confirmed the formation of oxalate precipitates when the phosphate ore leached with oxalic acid. The bands observed at broad over the range 3000–3500 cm^{-1} are attributed to the presence of the H—O—H stretchings of the crystal water of crystallization. Intense bands at 1614 and 1314 cm^{-1} are characterized bands to asymmetric and symmetric COO^- and specific to the calcium oxalate [43]. The strong peaks at 882, 864 cm^{-1} confirm the presence of C—C stretching vibrations due to the presence of $C_2O_4^{2-}$ in $CaC_2O_4{}^{\bullet}nH_2O_{(s)}$. Bands at 781 cm $^{-1}$ and the wideband at 662 cm $^{-1}$ can be attributed to the presence of O—C = O and the bending modes of the H_2O, respectively. Also, the peak at 517 cm^{-1} confirms the presence of a metal-oxygen bond. These spectra approve and confirm the formation and precipitate of solid hydrated calcium oxalate ($CaC_2O_4{}^{\bullet}nH_2O_{(s)}$) with lanthanide-oxalate crystals [43–45], where complexes of lanthanide-oxalate can be co-precipitated with hydrated calcium oxalate [46]. From the experimental data obtained, 0.4 M $C_2H_2O_4$ gives a higher %R of lanthanides with small amounts of the other impurities and was selected for further investigations.

For $C_4H_6O_6$, the acid concentration was ranged from 0.1–4.0 M at 35 °C with L/S mass ratio of 8/1 for 30.0 min. Fig. 7 shows that the recovery percentage (%R) of lanthanides was increased from 3.5% to 93.2% with 17.1% Ca as concentration increased from 0.1 to 2.5 M. Then, as the concentration increased the %R of lanthanides remained constant. These partially leaching of Ca (%R = 57.1%) may be explained by the dissolution of carbonate minerals using tartaric acid and the formation Ca-tartrate precipitates during the leaching processes as the following investigated reaction:

$$CaCO_3 + H_2C_4H_4O_6 \rightarrow CaC_4H_4O_6\downarrow + CO_2\uparrow + H_2O \quad (1)$$

This reaction may be considered as an irreversible reaction because the produced CO_2 is removed by stirring the leaching mixture during the leaching process [19].

Also, the leaching of the other constituents depends on the composition and the nature of the apatite ore. Zafar and Ashraf [18] suggest a simple mechanism to describe and understanding the selective leaching process of these impurities as follows [18];

$$M_3(PO_4)_{2(s)} + 6HX_{(aq)} \rightarrow 3MX_{2(aq)} + 2H_3PO_{4(aq)} \quad (2)$$

Therefore, the following reactions describe the leaching process of phosphate ore by tartaric acid can be investigated as:

$$Ca_3(PO_4)_{2(s)} + 3H_2C_4H_4O_{6(aq)} \rightarrow 3CaC_4H_4O_{6(aq)} + 2H_3PO_{4(aq)} \quad (3)$$

Also, the leaching of lanthanides can be investigated by the following simplest reaction:

$$2LnPO_{4(s)} + 3H_2C_4H_4O_{6(aq)} \rightarrow Ln_2(C_4H_4O_6)_{3(aq)} + 2H_3PO_{4(aq)} \quad (4)$$

Reactions (1–4) were investigated to explain the leaching process of phosphate ore by tartaric acid. The results obtained indicate to the leaching of the phosphate associated with the lanthanides and the net solubilization of lanthanides was modest [47]. The investigated simplest reaction (4) shows the mechanism of lanthanides recovered from the ore using tartaric acid and can be explained depending on the fact that the hydroxy-di-carboxylates such as tartrate tend to be too insoluble [48]. This can be attributed to the fact that the solubility of tartrate ($C_4H_4O_6{}^{-2}$) in this reaction is lower than the solubility of phosphate ($PO_4{}^{-3}$) and lanthanides tartrate are more stable than the phosphates at the chosen optimum conditions. Previous studies showed that the complex of lanthanides and ($C_4H_4O_6{}^{-2}$) has a high stability constant where the oxygen atoms, in both ionized carboxylic groups (–COO-) and in the hydroxyl groups, were involved in complex formation [49].

Therefore, the mechanism of the leaching process of phosphate ore by tartaric acid can be explained by the investigation of dissolution and re-precipitation of lanthanides and some impurities on the apatite surface, as shown in the SEM micrograph of the leaching residue, Fig. 8c. Fig. 9c illustrates the FTIR spectra of phosphate ore leached by 2.5 M $C_4H_6O_6$. The peaks that appear at over the range 3000–3500 cm^{-1} are assigned to O—H mode. The strong absorption band at 1582 cm^{-1} is due to the presence of C=O. The sharp absorption band about 1383 cm^{-1} results from anti-symmetric stretching C=O while the peak at about 1332 cm^{-1} is assigned to symmetric stretching C—O [50–52]. The band appears at 1281 cm^{-1} is assigned to C—H bending. The absorption band at about 1131 cm^{-1} is resulted from the vibrational modes of C—H. The sharp absorption peaks at 1061 cm^{-1} and the peak at 1016 cm^{-1} are due to out of plane O—H deformation with stretching vibrations of C—O, respectively. The various intensities absorption bands between 816 and 533 cm^{-1} result from calcium–oxygen bonding. These results confirm and approve the formation of calcium tartrate crystals [52] during the leaching of phosphate ore by tartaric acid and agree with the results obtained in this study. Therefore, 2.5 M tartaric acid gives a higher %R of lanthanides with small values of the other impurities and so it was selected to be the optimum concentration in this study.

The influence of $C_3H_6O_3$ concentration on the leaching of phosphate ore in the range of 0.1–2.5 M was investigated. The other parameters were fixed at 90 min with L/S mass ratio of 8/1 at 35 °C. The data obtained indicated that (%R) of lanthanides increased from 0.9% to 89.1% as concentration increases from 0.1 to 1.8 M with 58.9% Ca, Fig. 7. The %R of lanthanides remains constant while the recovery percentage of Ca increased to 64.5% with further increasing of acid concentration to 2.5 M. This may be attributed to the fact that with increasing in $C_3H_6O_3$ concentration, the polarity of the acidic O—H bond decreases the number of H^+ ions due to the decreasing amount of H_2O molecules in the medium [18,22,53].

The mechanism of the leaching processes of apatite ore with lactic acid can be expressed as the following [19,53];

$$CaCO_{3(s)} + 2CH_3CH(OH)COOH_{(aq)} \rightarrow Ca(CH_3CH(OH)COO)_{2(aq)} + CO_2 + H_2O \quad (5)$$

Eq. (5) can be regarded as an irreversible reaction where the produced CO_2 removed during the stirring of the ore -acid mixture [53].

The leaching mechanism of the other constituents depended on the composition and nature of the phosphate ore [19,53]. Therefore, the leaching of lanthanides from phosphate ore using lactic acid can be investigated as the following simplest reaction:

$$LnPO_{4(s)} + 3CH_3CH(OH)COOH_{(aq)} \rightarrow Ln(CH_3CH(OH)COO)_{3(aq)} + H_3PO_{4(aq)} \quad (6)$$

The reaction (6) was investigated to explain the recovery of lanthanides from phosphate ore by lactic acid under investigated optimum conditions. Previous works [16,53] have explained the ability of different organic acids to decompose phosphate ore. The results showed that the solubility rate of phosphate is affected not only by the pH of the media but also by the structural composition of the organic acid, which is considered as the most important parameter in attack the tricalcium phosphate [54]. Also, the number of hydroxyl groups per each acid molecule is an important factor that affects the dissolution of phosphate rate. The presence of more than one hydroxyl group (as in lactic acid) will increase the dissolution rate [54]. On the other hand, the stability lanthanide-lactate complex can be attributed to the fact that the complex is inner-sphere and lactate coordinates to lanthanides in a bidentate mode by two oxygen atoms, one of the carboxylate group and another of the protonated α-hydroxyl group [55]. Therefore, the solubility of lactate in the investigated reactions is lower than the solubility of phosphate.

The SEM micrograph of the residue obtained is represented in Fig. 8d, which ensures and reveals that selective leaching occurred with the lactic acid where the phosphate ore is attacked by the acid under the investigated conditions. Fig. 9d deduced that after acid leaching, the absorption bands of PO_4^{3-} groups at 472.6, 563.7, 964.4, and 1091.7 cm^{-1} and the characterized bands of CO_3^{2-} groups appearing at about 864 and 1429 cm^{-1} were decreased to values smaller than that observed for phosphate ore before leaching. Also, the peaks of carbonated fluoroapatite observed at 1458.2 cm^{-1} and the intensity of the other absorption bands characterized for the apatite ore were decreased to smaller values after leaching, as compared with those reported for ore before leaching with lactic acid.

XRD and FTIR data confirm and approve the experimental results obtained and ensure that selective leaching occurred by using lactic acid. From the experimental results, 1.8 M lactic acid gives a higher %R of lanthanides with small values of the other impurities and so it was selected to be the optimum concentration in this work.

Fig. 7 *shows the effect of H_2SO_4 concentration* ranged from 0.1 to 2.5 M on leaching percentage of lanthanides with L/S mass ratio of 5/1 at 25 °C for 150 min. It was observed that the (%R) of lanthanides reached to 89.3% and 12.7% Ca with increasing H_2SO_4 concentration to 2.0 M. This may be due to the fact that at a lower acid concentration, the amount of acid required to leach either lanthanides or calcium from the phosphate ore is insufficient. With a further increase in H_2SO_4 concentrations leaching percentages of lanthanides and calcium were decreased down. This may be due to the formation of $CaSO_4$ and re-precipitation of lanthanides [56].

The leaching reactions of the phosphate ore by H_2SO_4 can be described as in the following equations [57]:

$$Ca_{10}(PO_4)_6 \cdot CO_3 \cdot H_2O_{(s)} + 10H_2SO_4 + 18H_2O \rightarrow 10CaSO_4 \cdot 2H_2O_{(s)} + 6H_3PO_{4(l)} + CO_{2(g)} \quad (7)$$

The reaction between lanthanide ions in phosphate ore and sulfate ions in sulfuric acid to give $Ln_2(SO_4)_3$ can be written as the following reaction [57];

$$Ln^{3+} + SO_4^{2-} \leftrightarrow [LnSO_4]^+ \quad (8)$$

Where; Ln^{3+} is lanthanide ions with "+3" charge.

Therefore, the following reaction can be investigated:

$$2LnPO_4 + 3H_2SO_4 \leftrightarrow Ln_2(SO_4)_3 + 2H_3PO_4 \quad (9)$$

Different parameters affect the number of crystallization water molecules of $CaSO_4$ formed, Eq. (7), which can take values of 0, 0.5, or 2, such as the concentration of P_2O_5 in the phosphate ore and the reaction temperature [57].

The SEM micrograph of the residue obtained after leaching of phosphate ore by H_2SO_4 represented in Fig.8e confirms that calcium sulfate hydrates (gypsum) ($10CaSO_4{\cdot}2H_2O$), hemihydrate ($10CaSO_4{\cdot}1/2H_2O$), and anhydrite ($CaSO_4$)) are formed in the residue [57].

Fig. 9e illustrates the FTIR spectra of the residue of the phosphate ore leached by 2.0 M H_2SO_4. The bands appear in the range 1597–1795 and 3400–3500 cm^{-1} arises from the presence of H-O-H bending and H_2O molecules of gypsum and these data confirm the formation of gypsum [58]. Also the bands at 3580 and 3430 cm^1 are due to the presence of water molecules in the gypsum and $CaSO_4$ hemihydrate [58]. The two band assignments at 1683 and 1627 cm^{-1} suggest the presence of two crystallographic distinct types of H_2O molecules, one type associated with the SO_4^{2-} groups by hydrogen bond while the second type due to the direct bond between H_2O and calcium ions. The strong characteristic bands centered around 1200 cm^{-1} and the weak bands at 669.3 and 607.6 cm^{-1} is originated from the presence of SO_4^{2-}as in pure gypsum spectrum [59].

This phosphogypsum may contain lanthanides by isomorphous substitutions with Ca^{2+} [8], these may be due to they have similar ionic radii.

The data obtained by SEM and FTIR confirm and approve the data obtained in the leaching process of phosphate ore with 2.0 M H_2SO_4. So, the suitable H_2SO_4 concentration used in this study is selected to be 2.0 M and used for further investigations.

The effect of HCl concentration ranged from 0.1 to 4.0 M on the leaching of lanthanides and Ca from the phosphate ore was studied with an L/S ratio of 5/1 for 150 min at 35 °C. As in Fig. 7, the %R of lanthanides and calcium was reached to 74.6 % and 35.8%, respectively, at 3.0 M HCl. Then, the %R decreased with further increase in acid concentration to 4.0 M. These results can be attributed to the mineralogical structure of the apatite where the lanthanides ions are concentrated at the outer phosphate grain surface than at the center of the grains. Furthermore, the concentration of Ca gradually increases from the surface of the grains of the center [8].

At low HCl concentrations, mono-calcium phosphate can be formed according to the following [60];

$$Ca_{10}(PO_4)_6F_2 + 14HCl \rightarrow 10CaCl_2 + 6H_2PO_4^- + 2HF \quad (10)$$

H_3PO_4 will formed if high HCl concentration used, as the following reaction [59];

$$Ca_{10}(PO_4)_6F_2 + 20HCl \rightarrow 10CaCl_2 + + 2HF \quad (11)$$

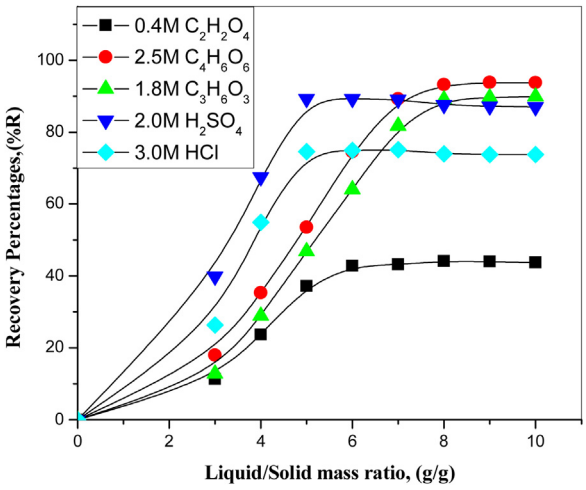

Fig. 10 – Effect of L/S mass ratio on the leaching of lanthanides from Phosphate ore with organic and inorganic acids.

H_3PO_4 formed in reaction (11) will react with phosphate ore to form $CaHPO_4$, which is insoluble in water [60];

$$Ca_{10}(PO_4)_6F_2 + 4H_3PO_4 \rightarrow 10CaHPO_4 + 2HF \quad (12)$$

Also, lanthanides can be leached from the ore as the following reaction [8];

$$LnPO_4 + 3HCl \rightarrow LnCl_3 + H_3PO_4 \quad (13)$$

The SEM micrograph of the residue obtained after the dissolution of phosphate ore by HCl represented in Fig. 8f, which confirm that calcium phosphate and calcium carbonate are precipitated as a residue.

The infrared spectrum of the residue is illustrated in Fig. 9f. The strong peak centered at 1024 cm^{-1} and the bands at about 473, 561, 580 and 964 cm^{-1} are attributed to the presence of phosphate groups in the residue. The bands that appear at 1193, 1118, and 1024 cm^{-1} can due to presence of OH-in plan-bending mode of $[HPO_4]^{-2}$ in the hydrated layer, stretching mode of $[HPO_4]^{-2}$ and PO_4^{-3}, and bands that appear at 598 and 561 cm^{-1} are due to bending mode of PO_4^{-3} [61]. The strong peak centered around 1429 cm^{-1} and the other bands at about 1454 and 864 cm^{-1} are characteristics of the CO_3^{-2}. Adsorbed water peak is relatively wide at 3600–2600 cm^{-1}. The data obtained SEM and FTIR confirm the experimental results obtained. From the experimental results, 3.0 M HCl gives a higher %R of lanthanides with small values of the other impurities and is investigated as the optimum concentration in this work.

3.2.3. *Effect of liquid/solid mass ratio*

The influence of liquid/solid (L/S) mass ratio on the leaching of lanthanides and calcium from phosphate ore with the investigated acids at chosen time and temperature was studied with 3/1 - 10/1 liquid/solid mass ratios. The results obtained are plotted and showed in Fig. 10. The experimental results show that the value of %R of lanthanides increased rapidly

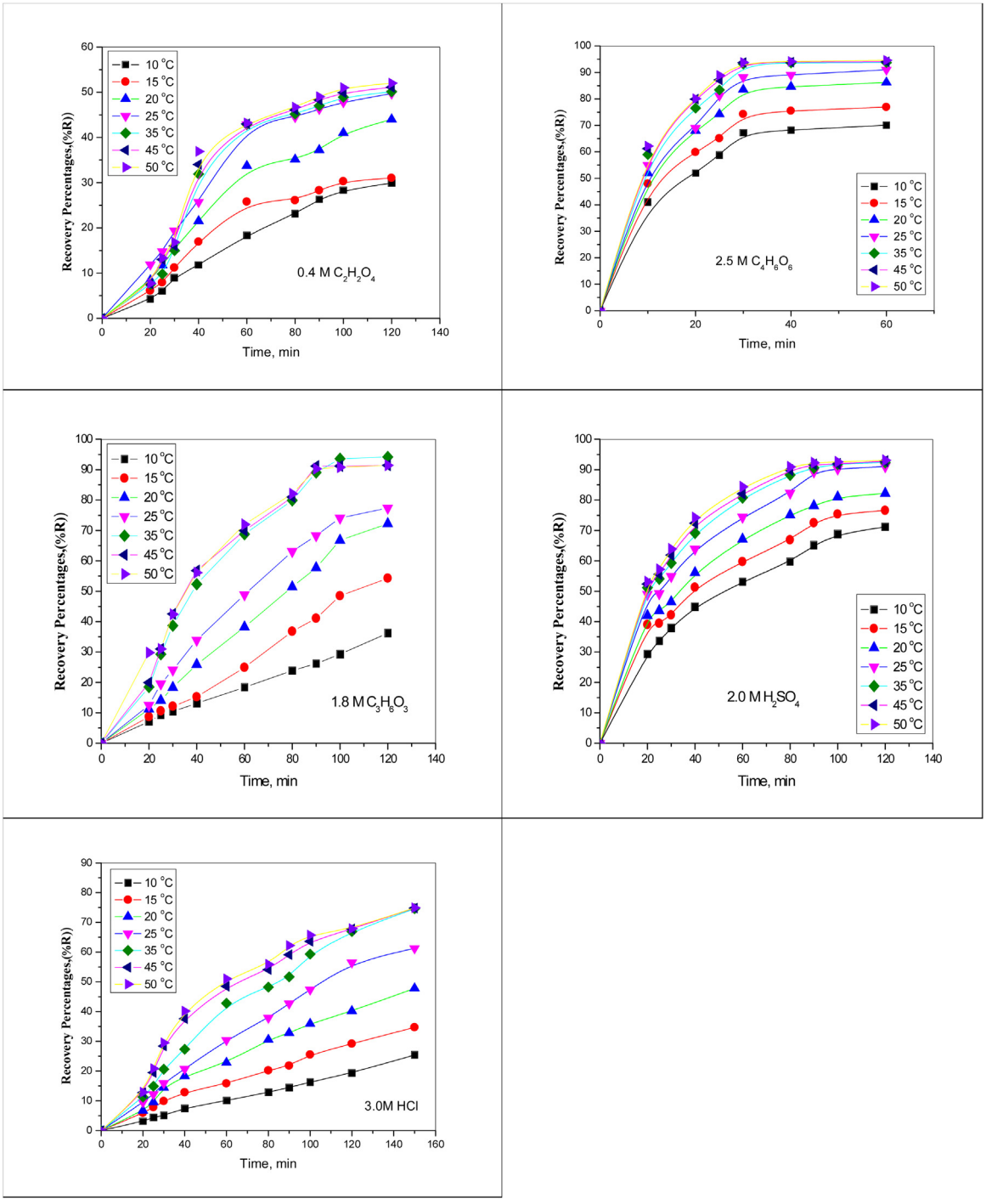

Fig. 11 – Effect of Temperature on the leaching of lanthanides from Phosphate ore with organic and inorganic acids with contact time.

as the liquid/solid (L/S) mass ratios increased to 5/1 (for both HCl and H_2SO_4), 6/1(for $C_2H_2O_4$), and 8/1 (for both $C_4H_6O_6$ and $C_3H_6O_3$), respectively. Under these conditions, the (%R) of lanthanides was 42.8%, 93.2%, 89.1%, 89.3% and 74.6% for $C_2H_2O_4$, $C_4H_6O_6$, $C_3H_6O_3$, H_2SO_4, and HCl, respectively. The lower values of (%R) at lower L/S mass ratios can be attributed to the insufficient acid concentration to leach a significant amount of lanthanides. With increasing the L/S mass ratio, the concentration of acid became sufficient to recover lanthanides from the phosphate rock. When the L/S mass ratio was higher than that recommended for each acid, the leaching of lanthanides slightly increased, while the leaching of other impurities was increased.

Therefore the recommended L/S mass ratio for each acid was chosen to give a higher recovery percentage of lanthanides with a small percentage of impurities and

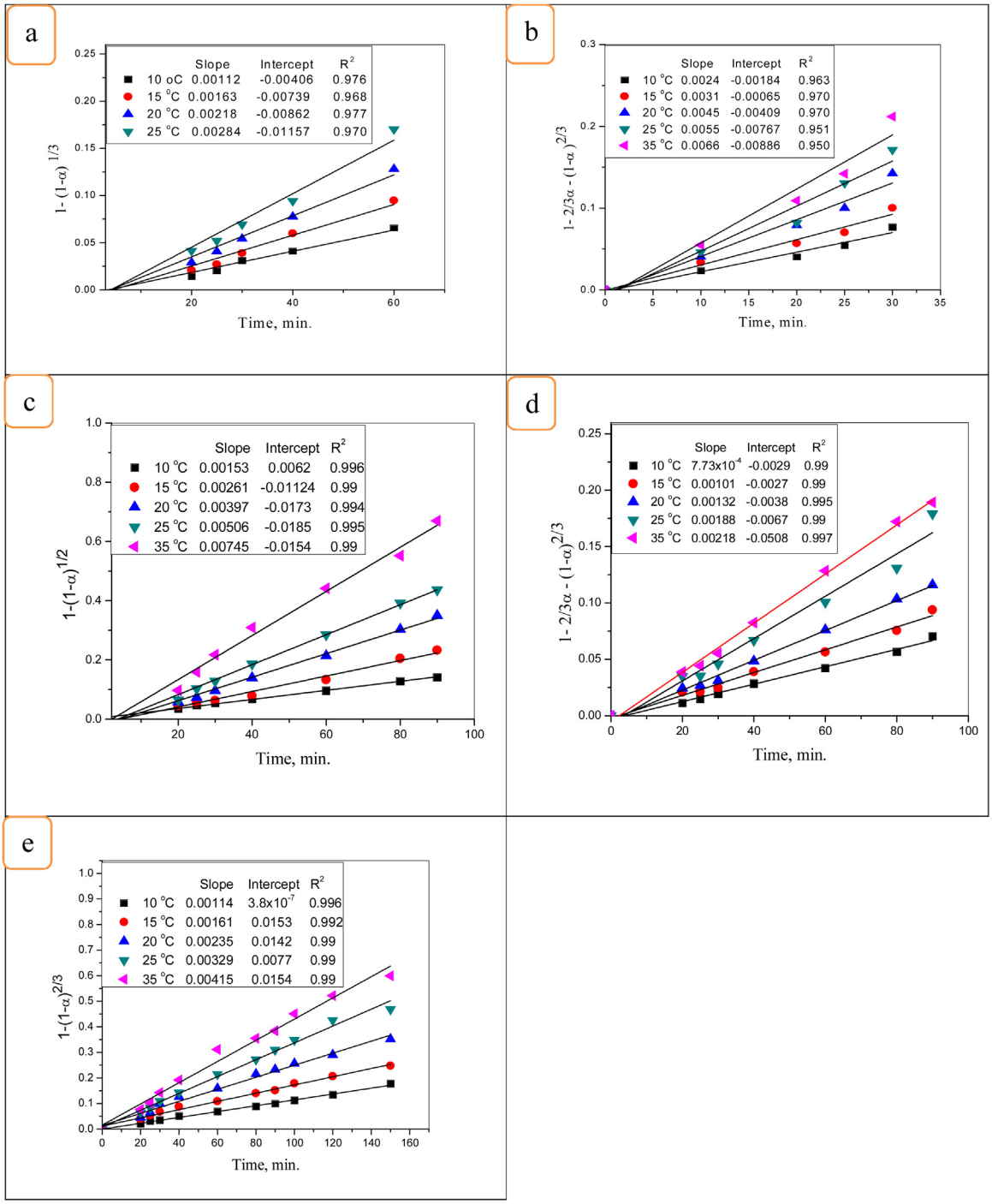

Fig. 12 – Plots of [1-(1- α)$^{1/3}$] for $C_2H_2O_4$ (a), [1-(1- α)$^{1/2}$] for $C_3H_6O_3$ (c), [1-(2/3)α-(1-α)$^{2/3}$] for both $C_4H_6O_6$ (b) and H_2SO_4 (d), and [1-(1- α)$^{2/3}$] for HCl(e), *vs.* time at various temperatures for the leaching of lanthanides from phosphate ore.

investigated as the optimum L/S mass ratio in our investigations.

3.2.4. *Effect of leaching temperature*

The influence of temperature on the recovery percentage of lanthanides from phosphate ore by the investigated acids was carried out at the temperature range 10–50 °C with time at the investigated optimum conditions. The results obtained, Fig. 11, shows that as the temperature increases to 25 °C, the %R of the lanthanides increased to 42.8% and 89.3% for $C_2H_2O_4$ and H_2SO_4, respectively. While at 35 °C, the %R of the lanthanides increased to 93.2%, 89.1% and 74.6% for $C_4H_6O_6$, $C_3H_6O_3$, and HCl, respectively. When temperature increases from 35 to 50 °C, the %R of lanthanide increased slowly. This can be attributed to the fact that both water and investigated organic acids tend to vaporize at higher temperatures, which leads to a decrease in the solubility of the reaction by-products in water. Therefore, the investigated leaching temperature is

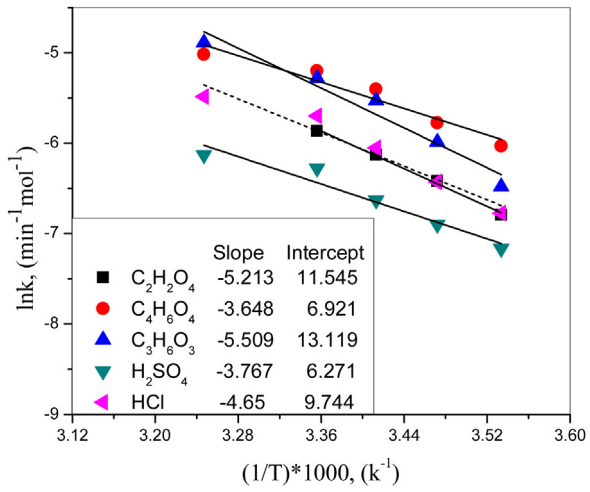

Fig. 13 – Arrhenius plot for leaching of lanthanides from phosphate ore by different acids.

more suitable for each investigated acid leaching process [19] to give a higher %R of lanthanides with a small value of impurities and investigated as the optimum temperature in this study.

Aqueous phase-separated from each acid leaching process was analyzed and chemical analyses of these solutions were found to contains variety in the recovery percentage of the lanthanides and other contaminants depending on the optimum conditions that were studied in our work for each acid leaching process, as the following:

- For $C_2H_2O_4$; 42.6% Ln, 12.8% Ca, 19.7% Fe, 11.3% Mg, 10.9% Al
- For $C_4H_6O_6$; 93.2% Ln, 17.1% Ca, 12.3% Fe, 8.8% Mg, 9.5% Al
- For $C_3H_6O_3$; 89.1% Ln, 58.9% Ca, 9.1 % Fe, 7.4% Mg, 6.9% Al
- For H_2SO_4; 89.3% Ln, 12.7% Ca 67.4 % Fe, 66.9% Mg, 63.2% Al
- For HCl; 74.6 %Ln, 35.8% Ca, 56.9% Fe, 49.8% Mg, 51.4% Al

3.2.5. *Kinetic analysis*

The experimental data obtained for each acid leaching process at different temperatures were analyzed to determine the kinetic parameters and rate-controlling step for investigated acid leaching processes of lanthanides from phosphate ore. The shrinking-core models were used to analyses these data to obtain the kinetic equation [62]. Based on the leaching conditions, type and nature solid materials, and the nature of leachant, the following standard equations describe shrinking-core kinetic models were investigated [18,19,62];

- Chemical reaction control dense shrinking spheres (or constant size) (Eq. 14), and cylindrical particles model (Eq. 15)

$$K_c t = [1 - (1-\alpha)^{1/3}] \quad (14)$$

$$K_c t = [1 - (1-\alpha)^{1/2}] \quad (15)$$

- The diffusion-controlled process through the inner layer

$$K_c t = [1 - \frac{2}{3}\alpha - (1-\alpha)^{2/3}] \quad (16)$$

- Ash diffusion control dense constant size-spherical particles

$$K_c t = [1 - 3(1-\alpha)^{2/3} + 2(1-\alpha)] \quad (17)$$

- Film diffusion control dense shrinking spheres

$$K_c t = [1 - (1-\alpha)^{2/3}] \quad (18)$$

where k_c = the reaction rate constant (min^{-1}), t = the reaction time (min), α = the fraction of the lanthanides leached from phosphate ore (% R/100).

The relationships between the experimental data obtained from the suggested kinetic models against time (min) were plotted and represented in Fig. 12. The results showed that experimental data fit with chemical reaction control models $[1-(1-\alpha)^{1/3}]$ leaching processes of ore by $C_2H_2O_4$ (a) and $[1-(1-\alpha)^{1/2}]$ for $C_3H_6O_3$(c), and fit with the diffusion-controlled process through the inner layer $[1-(2/3)\alpha-(1-\alpha)^{2/3}]$ for the leaching of phosphate ore by both $C_4H_6O_6$ (b) and H_2SO_4 (d), and $[1-(1-\alpha)^{2/3}]$ for HCl(e). These models equations have been selected depending on the highest value of R^2, *i.e.* Eq.s (14–18) have been selected and found to give a straight line with plotting *vs.* time (t) at different leaching temperatures with a good correlation $R^2 \geq 0.99$.

The activation energy (E_a) required to the lanthanides leached from phosphate ore by the investigated acids under the optimum conditions was calculated by using the following Arrhenius equation:

$$K = A \exp\left(\frac{-E_a}{RT}\right) \quad (19)$$

Table 3 – Comparison of leaching processes using the investigated acids.

Factor/ Acid	Leaching time, min.	Acid Conc., (M)	L/S mass ratio	T, °C	%R	E ($kJmol^{-1}$)	Ref.
$H_2C_2O_4$	60	0.4	6/1	25	42.8	43.3	This work
$C_4H_6O_6$	30	2.5	8/1	35	93.2	30.33	This work
$C_3H_6O_3$	90	1.8	8/1	35	89.1	45.8	This work
	60	1.0	5/1	20	85	Not detected	[52]
H_2SO_4	300	5.0	9/1	20	90	Not detected	[8]
	90	2.0	5/1	25	89.3	31.3	This work
HCl	120	2.0	9/1	20	≈ 100	Not detected	[8]
	150	3.0	5/1	35	74.6	38.26	This work

Where A is the frequency factor, E_a is the activation energy of the reaction, R is the universal gas constant (8.314 Jk^{-1} mol^{-1}), and T is absolute temperature, k. The values of apparent rate constant (K) for each acid were calculated as the slopes of the straight lines obtained in Fig. 12. The calculated values of (lnK) were plotted against 1/T to give straight lines with a slope of ($-E_a$/RT) and an intercept of (lnA) as shown in Fig. 13.

The activation energy for each acid leaching process under the investigated temperature range was calculated to be 43.3, 30.33, 45.8, 31.3, and 38.6 kJmol^{-1} for $C_2H_2O_4$, $C_4H_6O_6$, $C_3H_6O_3$, H_2SO_4, and HCl, respectively.

3.3. *Comparison of leaching processes using the investigated acids*

The experimental results obtained in the leaching processes by $C_2H_2O_4$, $C_4H_6O_6$, $C_3H_6O_3$, H_2SO_4, and HCl are showed and compared with other studies in Table 3. The results obtained illustrate that the leaching processes of lanthanides under the optimum condition has the order of;

$$C_4H_6O_6 > H_2SO_4 \geq C_3H_6O_3 > HCl > C_2H_2O_4$$

It is observed that the preferential leaching of lanthanides from the phosphate ore was obtained by using 2.5 M $C_4H_6O_6$ solution compared with the other leaching agents used in this study under the investigated optimum conditions and those of reported in the literature [8,52].

4. Summary and conclusions

In order to leach lanthanides from Al-Jalamide phosphate ore, different acids leaching processes were investigated and studied. The leaching processes were carried out using some organic and inorganic acids such as $C_2H_2O_4$, $C_4H_6O_6$, $C_3H_6O_3$, H_2SO_4, and HCl. Different experiments were carried on to characterize the phosphate ore before and after (residue) each leaching process such as XRF, SEM, XRD, and IR. The leaching percentage of lanthanides was found to increase with increasing leaching time, acid concentration, L/S mass ratio and temperature. The optimal leaching conditions were determined as 0.4 M $H_2C_2O_4$, 2.5 M $C_4H_6O_6$, 1.8 M $C_3H_6O_3$, 2.0 M H_2SO_4, and 3.0 M HCl, with a L/S ratio of 6/1 $H_2C_2O_4$, 8/1 for both $C_4H_6O_6$ and $C_3H_6O_3$, and 5/1 for both H_2SO_4, and HCl at 30 °C with agitation rate ≈ 350 rpm and particle size fraction under ≈ 144.8 μm. Under the investigated optimum conditions, the leaching percent was 42.8%, 93.2%, 89.1%, 89.3%, and 74.6%, for $C_2H_2O_4$, $C_4H_6O_6$, $C_3H_6O_3$, H_2SO_4, and HCl, respectively. The mechanism of lanthanides leaching from phosphate ore under the investigated conditions was found to be chemically controlled with models of [1-(1- α)$^{1/3}$] and [1-(1- α)$^{1/2}$] for the leaching processes of ore by $C_2H_2O_4$ and $C_3H_6O_3$ with activation energies of 43.3 and 45.8 kJ mol^{-1}, respectively, and [1-(1- α)$^{2/3}$] for HCl with an activation energy of 38.6 kJmol^{-1}, diffusion-controlled process through the inner layer [1-(2/3)α-(1-α)$^{2/3}$] for the leaching of phosphate ore by $C_4H_6O_6$ and H_2SO_4 with activation energies of 30.33 and 31.3 kJ mol^{-1}, respectively. All the experimental data were confirmed and explained by XRD and FTIR.

Conflict of interest

The authors declare no conflicts of interest.

Acknowledgment

This work has been carried out within the framework of a project number (623/39) financed by the Jouf University during the year 1439 to 1440 H.

Appendix A. Supplementary data

Supplementary material related to this article can be found, in the online version, at doi:https://doi.org/10.1016/j.jmrt.2020.07.007.

REFERENCES

[1] Binnemans K, Jones PT, Blanpain B, Van Gerven T, Pontikes Y. Towards zero-waste valorization of rare-earth-containing industrial process residues: a critical review. J Clean Prod 2015;99:17–38, http://dx.doi.org/10.1016/j.jclepro.2015.02.089.

[2] Shin D, Kim J-S, Kim B, Jeong J, Lee J-C. Use of phosphate solubilizing bacteria to leach rare earth elements from monazite-bearing ore. Minerals 2015;5:189–202, http://dx.doi.org/10.3390/min5020189.

[3] Demir S, Brune NK, Van Humbeck JF, A. Mason JA, Plakhova TV, Wang S, et al. Extraction of lanthanide and actinide ions from aqueous mixtures using a carboxylic acid-functionalized porous aromatic framework. ACS Cent Sci 2016;2:253–65, http://dx.doi.org/10.1021/acscentsci.6b00066.

[4] Roy C, Knudsen BP, Pedersen CM, Velázquez-Palenzuela A, Christensen LH, Damsgaard CD, et al. Scalable synthesis of carbon supported platinum - lanthanide and rare earth alloys for oxygen reduction. ACS Catal 2018;8(3):2071–80, http://dx.doi.org/10.1021/acscatal.7b03972.

[5] Kusrini E, Nurani Y, Bahari ZJ. Extraction of rare earth elements from low-grade Bauxite via precipitation reaction. Materials Sci. Eng 2018;334:012052, http://dx.doi.org/10.1088/1757-899X/334/1/012052.

[6] Soltani F, Abdollahy M, Javad Koleini SM, Moradkhani D. Selection of an appropriate leaching method for light REEs from Esfordi flotation concentrate based on mineral characterization. J. Southern Africa Inst Mining Metallurg 2017;117:443–50, http://dx.doi.org/10.17159/2411-9717/2017/v117n5a6.

[7] Habashi F. The recovery of the lanthanides from phosphate rock. J Chem Tech Biotechnol 1985;35A:5–14, http://dx.doi.org/10.1002/jctb.5040350103.

[8] Kim R, Cho H, Han Kenneth N, Kim K, Mun M. Optimization of acid leaching of rare-earth elements from mongolian apatite-based ore. Minerals 2016;6(3):63–77, http://dx.doi.org/10.3390/min6030063.

[9] Chi R, Tian J, Zhu G, Wu Y, Li S, Wang C, et al. Kinetics of rare earth leaching from a mangnese-removed weathered rare-earth mud in hydrochloric acid solutions. Separ Sci Technol 2006;41:1099–113, http://dx.doi.org/10.1080/01496390600632503.

[10] Battsengel A, Batnasan A, Narankhuu A, Haga K, Watanabe Y, Shibayama A. Recovery of light and heavy rare earth elements from apatite ore using sulphuric acid leaching, solvent extraction and precipitation. Hydrometallurgy

2018;179:100–9, http://dx.doi.org/10.1016/j.hydromet.2018.05.024.
[11] Stone K, Bandara AMTS, Senanayake G, Jayasekera S. Processing of rare earth phosphate concentrates: a comparative study of pre-leaching with perchloric, hydrochloric, nitric and phosphoric acids and deportment of minor/major elements. Hydrometallurgy 2016;163:137–47, http://dx.doi.org/10.1016/j.hydromet.2016.03.014.
[12] Demol J, Ho E, Soldenhoff K, Senanayake G. The sulfuric acid bake and leach route for processing of rare earth ores and concentrates: a review. Hydrometallurgy 2019;188:123–39, http://dx.doi.org/10.1016/j.hydromet.2019.05.015.
[13] Senanayake G, Jayasekera S, Bandara AMTS, Koenigsberger E, Koenigsberger L, Kyle J. Rare earth metal ion solubility in sulphate-phosphate solutions of pH range− 0.5 to 5.0 relevant to processing fluorapatite rich concentrates: effect of calcium, aluminium, iron and sodium ions and temperature up to 80° C. J. Miner Eng 2016;98:169–76, http://dx.doi.org/10.1016/j.mineng.2016.07.022.
[14] Habashi F. Extractive metallurgy of rare earths. J. Canad Metallurg Quart 2013;52:224–33, http://dx.doi.org/10.1179/1879139513Y.0000000081.
[15] Case M, Fox R, Baek D, Wai C. Extraction of rare earth elements from chloride media with tetrabutyl diglycolamide in 1-octanol modified carbon dioxide. Metals 2019;9:429–44, http://dx.doi.org/10.3390/met9040429.
[16] Jorjani E, Bagherieh AH, Chelgani SC. Rare earth elements leaching from Chadormalu apatite concentrate: laboratory studies and regression predictions. Korean J Chem Eng 2011;28:557–62, http://dx.doi.org/10.1007/s11814-010-0383-4.0.
[17] Lazo DR, Dyer LG, Alorro RD, Browner R. Treatment of monazite by organic acids II: rare earth dissolution and recovery. Hydrometallurgy 2018;179:94–9, http://dx.doi.org/10.1016/j.hydromet.2018.05.022.
[18] Oral L, Bunyamin D, Fatih D. Dissolution kinetics of natural magnesite in acetic acid solutions. Inter J Mineral Process 2005;75:91–9, http://dx.doi.org/10.1016/j.minpro.2004.05.002.
[19] Zafar ZI, Ashraf M. Selective leaching kinetics of calcareous phosphate rock in lactic acid. Chem Eng J 2007;131:41–8, http://dx.doi.org/10.1016/j.cej.2006.12.002.
[20] Gharabaghi M, Irannajad M, Noaparast M. A review of the beneficiation of calcareous phosphate ores using organic acid leaching. Hydrometallurgy 2010;103:96–107, http://dx.doi.org/10.1016/j.hydromet.2010.03.002.
[21] Ashraf M, Zafar ZI, Ansari TM. Selective leaching kinetics and upgrading of low-grade calcareous phosphate rock in succinic acid. Hydrometallurgy 2005;80(4):286–92, http://dx.doi.org/10.1016/j.hydromet.2005.09.001.
[22] Demir F, Dönmez B, Çolak S. Leaching kinetics of magnesite in citric acid solutions. J. Chem. Eng. Japan 2003;36(6):683–8, http://dx.doi.org/10.1252/jcej.36.683.
[23] Martin P, Carlot G, Chevarier A, Den-Auwer C, Panczer G. Mechanisms involved in thermal diffusion of rare earth elements in apatite. J Nucl Phys Mater Sci Radiat Appl 1999;275:268–76, http://dx.doi.org/10.1016/S0022-3115(99)00126-9.
[24] Neser C. Future Phosphate Developments in Saudi Arabia. 2004 IFA Production and Trade Conference, October 3-5(2004) Dubai, UAE.
[25] Abouzeid AZM. Physical and thermal treatment of phosphate ores—an overview. Inter J Min Proc 2008;85:59–84, http://dx.doi.org/10.1016/j.minpro.2007.09.001.
[26] Zheng X, Smith RW. Dolomite depressants in the flotation of apatite and collophane from dolomite. Min Eng 1997;10(5):537–45, http://dx.doi.org/10.1016/S0892-6875(97)00031-9.
[27] Al-Fariss TF, Ozbelge HO, El-Shall HS. On the phosphate rock beneficiation for the production of phosphoric acid in Saudi Arabia. J King Saud Uni Eng Sci 1992;4(l):13–32, http://dx.doi.org/10.1016/S1018-3639(18)30553-1.
[28] Al-Fariss TF, Ozbelge HO, Abdulrazik AM. Optimum flotation condition for AI-Jalamid. Phosphate rock. Dev Chem Eng Miner Process 1993;1(1):56–62, http://dx.doi.org/10.1002/apj.5500010107.
[29] Wua S, Wang L, Zhao L, Zhang P, El-Shall H. Recovery of rare earth elements from phosphate rock by hydrometallurgical processes – a critical review. Chem Eng J 2018;335:774–800, http://dx.doi.org/10.1016/j.cej.2017.10.143.
[30] Marczenko Z. Specrtophotometric determination of elements. New York: Johon Wiley and sons, Inc.; 1986. p. 438, http://dx.doi.org/10.1016/j.cej.2017.10.143.
[31] Chi R, Tian J, Zhu G, Wu Y, Li S, Wang C, et al. Kinetics of rare earth leaching from a mangnese-removed weathered rare-earth mud in hydrochloric acid solutions. Sep Sci Tech 2006;41:1099–113, http://dx.doi.org/10.1080/01496390600632503.
[32] Eisa MY, Al Dabbas M, Abdulla FH. Quantitative identification of phosphate using X-Ray diffraction and Fourier transform infra red (FTIR) spectroscopy. Int J Curr Microbiol App Sci 2015;4(1):270–83.
[33] Raynaud S, Champion E, Bernache-Assollant D, Laval J-P. Determination of calcium/phosphorus atomic ratio of calcium phosphate apatites using X-ray diffractometry. J Am Ceram Soc 2001;84(2):359–66, http://dx.doi.org/10.1111/j.1151-2916.2001.tb00663.x.
[34] Markovic M, Fowler BO, Tung MS. Preparation and comprehensive characterization of a calcium hydroxyapatite reference material. J Res Natl Inst Stand Technol 2004;109(6):553–68, http://dx.doi.org/10.6028/jres.109.042.
[35] Tchangbeddji G, Djeteli G, Kili KA, Savariault JM, Lacout JL. Chemical and structural characterization of natural phosphate of hahotoe (Togo). Bull Chem Soc Ethiop 2003;17(2):139–46, http://dx.doi.org/10.4314/bcse.v17i2.61659.
[36] Zhang Q, Qiu Y, Cao J, Wang Y, Hu J, et al. Study on the rare earth containing phosphate rock in guizhou and the way to concentrate phosphate and rare earth metal thereof. J Powder Metall Min 2014;3(2):126–9, http://dx.doi.org/10.4172/2168-9806.1000126.
[37] Halcomb DW, Young RA. Thermal decomposition of human tooth enamel. Calcified Tissue Int 1980;31:189–201, http://dx.doi.org/10.1007/BF02407181.
[38] Uçuruma M, Toramana ÖY, Depcib T, Yoğurtçuoğlua E. A study on characterization and use of flotation to separate unburned carbon in bottom ash from cayirhan power plant. Energy Sources Part A Recovery Util Environ Eff 2001;33:562–74, http://dx.doi.org/10.1080/15567030903117638.
[39] Elouear Z, Bouzid J, Boujelben N, Feki M, Jamoussi F, Montiel A. Heavy metal removal from aqueous solutions by activated phosphate rock. J Hazard Mater 2008;156:412–20, http://dx.doi.org/10.1016/j.jhazmat.2007.12.036.
[40] Chaabouni A, Chtara C, Nzihou A, El Feki H. Textural and mineralogical studies of two tunisian sedimentary phosphates or carbonated fluorapatite used in the process of production of phosphoric acid. Inter J Sci Tech Res 2016;5:161–6.
[41] Al-Fariss TF, Abd El-Aleem FA, El-Nagdy KA. Beneficiation of Saudi phosphate ores by column flotation technology. J King Saud Univ Eng Sci 2013;25:113–7, http://dx.doi.org/10.1016/j.jksues.2012.05.002.
[42] Song J, Zhu G, Zhang P, Zhao Y. Reduction of low-grade manganese oxide ore by biomass roasting. Acta Metall Sin (Engl Lett) 2010;23(3):223–9 http://www.amse.org.cn/EN/Y2010/V23/I3/223.

[43] Keith W, Goyne Susan L, Chorover BJ. Effects of organic acids and dissolved oxygen on apatite and chalcopyrite dissolution: implications for using elements as organomarkers and oxymarkers. Chem Geol 2006;234:28–45, http://dx.doi.org/10.1016/j.chemgeo.2006.04.003.
[44] Neaman A, Chorover J, Brantley SL. Implications of the evolution of organic acid moieties for basalt weathering over geologic time. Am J Sci 2005;305:147–85.
[45] Bouropoulos C, Vagenas N, Klepetsanis P, Stavropoulos N, Bouropoulos N. Growth of calcium oxalate monohydrate on uric acid crystals at sustained supersaturation. Crystal Res. Technol 2004;39(8):699–704, http://dx.doi.org/10.1002/crat.200310241.
[46] John MV, Ittyachen M. Growth and characterization of cerium lanthanum oxalate crystals gown in hydro-silica gel. Cryst Res Technol 2001;36:141–6, http://dx.doi.org/10.1002/1521-4079(200102)36:2&141::AID-CRAT141&3.0.CO;2-0.
[47] Lapidus GT, Doyle FM. Selective thorium and uranium extraction from monazite: i. Single-stage oxalate leaching. Hydrometallurgy 2015;154:102–10, http://dx.doi.org/10.1016/j.hydromet.2015.04.00.
[48] Mills DJ, Kambah. Removal of phosphate from water, Sep. 20, 2005, Patent No.: US 6,946,076 B2.
[49] Riri M, Hor M, Serdaoui F, Hlaibi M. Complexation of trivalent lanthanide cations by different chelation sites of malic and tartric acid (composition, stability and probable structure). Arabian J Chem 2016;9:S1478–86, http://dx.doi.org/10.1016/j.arabjc.2012.03.012.
[50] Xu W, Chang HS, Liu W, Zheng YQ. Synthesis, crystal structure, and properties of a new lanthanide tartrate coordination polymer. Russian J Coord Chem 2014;40(40):251–6, http://dx.doi.org/10.1134/S1070328414030105.
[51] Nakamot K. Infrared and raman spectra of inorganic and coordination compounds, Pt. B. New York: Interscience Wiley; 2009.
[52] Parekh BB, Joshi VS, Pawar V, Thaker VS, Joshi MJ. *Aspergillums Niger* assisted crystal growth of calcium tartrate: an alternative method to grow crystals. Cryst Res Tech 2009;44:31, http://dx.doi.org/10.1002/crat.200800405.
[53] Heydarpour T, Rezai B, Gharabaghi M. A kinetics study of the leaching of a calcareous phosphate rock by lactic acid. Chem Eng Res Des 2011;89:2153–8, http://dx.doi.org/10.1016/j.cherd.2010.12.011.
[54] Lazo DE, Dyer LG, Alorro RD. Silicate, phosphate and carbonate mineral dissolution behaviour in the presence of organic acids: a review. Miner Eng 2017;100:115–23, http://dx.doi.org/10.1016/j.mineng.2016.10.013.
[55] Tian G, Martin LR, Rao L. Complexation of lactate with neodymium(iii) and europium(iii) at variable temperatures: studies by potentiometry, microcalorimetry, optical absorption, and luminescence spectroscopy. Inorg Chem 2010;49(22):10598–605, http://dx.doi.org/10.1021/ic101592h.
[56] Battsengel A, Batnasan A, Narankhuu A, Haga K, Watanabe Y, Shibayama A. Recovery of light and heavy rare earth elements from apatite ore using sulphuric acid leaching, solvent extraction and precipitation. Hydrometallurgy 2018;179:100–9, http://dx.doi.org/10.1016/j.hydromet.2018.05.024.
[57] Sevim F, Saracü H, Kocakerim MM, Yartasüi A. Dissolution kinetics of phosphate ore in H_2SO_4 solutions. Ind Eng Chem Res 2003;42:2052–7, http://dx.doi.org/10.1021/ie020168o.
[58] Singh M, Rajesh VJ, Kannan B, Bhattacharya S. Spectral and chemical characterization of gypsum-phyllosilicate association in Tiruchirapalli, South India, and its implications. Geological J 2018;53(5):1685–97, http://dx.doi.org/10.1002/gj.2990.
[59] Boke H, Akkurt S, Ozdemir S, Gokturk EH, Saltik ENC. Quantification of $CaCO_3$ -$CaSO_3$.0.5H_2O-$CaSO_4$. 2H_2O mixtures by FTIR analysis and its ANN model. Matt Lett 2004;58(5):723–6, http://dx.doi.org/10.1016/j.matlet.2003.07.008.
[60] Shlewit H. Treatment of phosphate rocks with hydrochloric acid. J Radioanal Nucl Chem 2011;287:49–54, http://dx.doi.org/10.1007/s10967-010-0687-1.
[61] Yokoi T, Kamitakahara M, Kawashita M, Ohtsuki C. Formation of organically modified octacalcium phosphate in solutions containing various amounts of benzenedicarboxylic acids. J Ceram Soc Jap 2013;121(2):219–25, http://dx.doi.org/10.2109/jcersj2.121.219.
[62] Levenspiel O. Chemical reaction engineering. 2nd ed New York: John Wiley; 1999.